J Fluoresc
DOI 10.1007/s10895-015-1719-6

ORIGINAL ARTICLE

Synthesis, Characterization and Fluorescence Properties of Zn(II) and Cu(II) Complexes: DNA Binding Study of Zn(II) Complex

Parirokh Lavaee[1] · Hossein Eshtiagh-Hosseini[1] · Mohammad Reza Housaindokht[1] · Joel T. Mague[2] · Abbas Ali Esmaeili[1] · Khalil Abnous[3]

Received: 8 September 2015 / Accepted: 28 October 2015

Abstract Zinc(II) and copper(II) complexes containing Schiff base, 2- methoxy-6((E)-(phenylimino) methyl) phenol ligand (HL) were synthesized and characterized by elemental analysis, IR, NMR, and single crystal X-ray diffraction technique. The fluorescence properties and quantum yield of zinc complex were studied. Our data showed that Zn complex could bind to DNA grooves with $K_b = 10^4\ M^{-1}$. Moreover, Zn complex could successfully be used in staining of DNA following agarose gel electrophoresis. MTT assay showed that Zn complex was not cytotoxic in MCF-7 cell line. Here, we introduce a newly synthesized fluorescence probe that can be used for single and double stranded DNA detection in both solution and agarose gels.

Keywords Copper · Zinc · Schiff base · Interaction · DNA · Fluorescence

Electronic supplementary material The online version of this article (doi:10.1007/s10895-015-1719-6) contains supplementary material, which is available to authorized users.

✉ Hossein Eshtiagh-Hosseini
heshtiagh@um.ac.ir

[1] Department of Chemistry, Faculty of Science, Ferdowsi University of Mashhad, Mashhad 917751436, Iran

[2] Department of Chemistry, Tulane University, New Orleans, LA 70118, USA

[3] Pharmaceutical Research Center, School of Pharmacy, Mashhad University of Medical Sciences, Mashhad, Iran

Introduction

Schiff base ligands have important role in coordination chemistry field with some advantages like easy synthesis and accessibility of starting materials [1–3]. Recently, Schiff base derived ligands and their complexes are shown to have biological applications such as antibacterial and antitumor activities [4–9]. Some of these compounds are used as fluorophores with analytical applications as well as in biosensor fabrications [10, 11]. Schiff base ligands have also been used in organic light emitting diodes [OLED] [12]. Coordination with metals, through N an O atoms, may induce or increase fluorescence of Schiff base ligands by increasing rigidity of complex [3, 12].

Zinc and copper coordinated compounds have potential applications in the field of luminescence, nonlinear optics and catalyst [13, 14]. Although Zn(II) ion has not optical characteristics because of its closed shell $3d^{10}$, it can enhance fluorescence of ligands upon coordination [3, 12]. In contrast, copper decrease or quench fluorescence of ligands due to its odd electron number in balance shell [15].

DNA can non-covalently interact with other molecules in three ways: (1) electrostatic interactions through the negatively charged phosphate backbone, (2) interaction of molecules with the minor and major grooves of DNA double helix, causing little perturbation of DNA structure, and (3) intercalation by inserting aromatic rings between the stacked base pairs of double-stranded DNA; with intercalating agents being the strongest one [16, 17]. Hydrogen bonding and hydrophobic interactions enhance DNA binding affinity in intercalating agents [18].

Published online: 04 November 2015

Table 1 Crystal and refined data of Zn and Cu complexes

Compound	Cu complex	Zn complex
Chemical formula	$C_{28}H_{24}CuN_2O_4$	$C_{28}H_{24}N_2O_4Zn$
Formula weight	516.03	517.86
Crystal system	monoclinic	triclinic
Temperature	150(2) K	95(2) *K*
Space group	*C*2/*c*	*P* − 1
Unit cell Dimensions	*a* = 14.6771(12) Å *b* = 12.9262(10) Å *c* = 13.6657(11) Å *β* = 114.9320(11)°	*a* = 9.4331(3) Å *b* = 11.1797(4) Å *c* = 12.8613(5) Å *α* = 69.3130(13)° *β* = 70.3640(13)° *γ* = 70.2810(11)°
Volume	2351.0(3) $Å^3$	1157.70(7) $Å^3$
Z	4	2
Density (calculated)	1.458 g/cm^3	1.486 g/cm^3
Absorption coefficient	0.967 mm^{-1}	1.794 mm^{-1}
F(000)	1068	536
θ(°)	2.20 to 29.58°	3.79 to 72.32°
*R*1	0.0399	0.0355
w*R*2 (all data)	0.0878	0.0758
GOF on F^2	1.069	1.062
Index ranges	$-20 \le h \le 19$ $-17 \le k \le 17$ $-18 \le l \le 18$	$-11 \le h \le 11$ $-13 \le k \le 13$ $-15 \le l \le 15$

Table 2 Select bond lengths [Å] and angles [°] for complexes

Complex			
Cu complex			
Cu1-O1	1.8984(11)	Cu1-O1	1.8984(11)
Cu1-N1	1.9585(12)	Cu1-N1	1.9585(12)
O1-C1	1.3065(19)	O2-C2	1.369(2)
O2-C8	1.428(2)	N1-C7	1.3003(19)
N1-C9	1.4317(19)	C1-C6	1.417(2)
O1-Cu1-O1	141.74(8)	O1-Cu1-N1	94.86(5)
O1-Cu1-N1	95.11(5)	O1-Cu1-N1	95.11(5)
O1-Cu1-N1	94.86(5)	N1-Cu1-N1	149.25(8)
C1-O1-Cu1	124.27(10)	C2-O2-C8	116.63(14)
C7-N1-C9	119.58(13)	C7-N1-Cu1	121.79(11)
C9-N1-Cu1	118.48(10)	O1-C1-C6	124.81(14)
O1-C1-C2	118.13(14)	C6-C1-C2	117.06(14)
O2-C2-C3	124.34(15)	O2-C2-C1	114.22(14)
Zn complex			
Zn1-O1	1.9130(14)	Zn1-O3	1.9254(15)
Zn1-N2	2.0113(16)	Zn1-N1	2.0289(18)
O1-C1	1.306(2)	O2-C2	1.371(3)
O2-C7	1.426(3)	O3-C15	1.313(2)
O4-C16	1.388(2)	O4-C21	1.423(3)
N1-C8	1.300(3)	N1-C9	1.428(3)
N2-C22	1.297(3)	N2-C23	1.429(3)
O1-Zn1-O3	116.09(6)	O1-Zn1-N2	121.57(6)
O3-Zn1-N2	95.57(6)	O1-Zn1-N1	96.24(6)
O3-Zn1-N1	128.03(7)	N2-Zn1-N1	100.70(7)
C1-O1-Zn1	125.13(13)	C2-O2-C7	117.20(16)
C15-O3-Zn1	125.56(13)	C16-O4-C21	115.77(17)
C8-N1-C9	119.31(18)	C8-N1-Zn1	120.69(15)
C9-N1-Zn1	119.93(13)	C22-N2-C23	118.85(17)
C22-N2-Zn1	122.15(14)	C23-N2-Zn1	118.52(13)
O1-C1-C6	125.80(19)	O1-C1-C2	117.51(18)
C6-C1-C2	116.68(18)	O2-C2-C3	124.23(19)

Intercalating fluorescence probes, including organic dyes, metal ions and metal complexes, can potentially be used as therapeutic and diagnostic agents and they are frequently employed to investigate nucleic acid and develop novel non-radioactive probes of DNA structure [19–23].

In this context, we synthesized zinc(II) and copper(II) complexes containing Schiff base, 2- methoxy-6 ((E)-(phenylimino) methyl) phenol ligand (HL). Crystal structure and fluorescence properties before and after complex formation were reported. Interaction of the newly synthesized inorganic complexes with ddDNA has also been examined. Fluorescence properties of these compounds after binding to DNA were studied. Moreover, Zn complex was successfully used to stain DNA agarose gel.

Experimental

Materials and Methods

O-vanillin was purchased from Sigma and other reagents and solvents were provided from Merck. Salmon sperm DNA (Invitrogen, USA) was dissolved in Tris HCl buffer solution 10 mM (pH 7.0). Concentration of DNA was determined by measuring A_{260} and assuming the molar extinction coefficient to be 6600 $M^{-1}cm^{-1}$. All experiments were performed using Milli-Q deionized water.

Instrumentation

Elemental analysis (C, H, and N) were carried out on Costech ECS 4010 CHNS Elemental Analyzer. The FT-IR spectra of complexes were recorded from 4000 to 400 cm^{-1} (Spectrum Two IR Spectrometers Perkin Elmer), NMR spectra were recorded in DMSO-*d6* at room temperature on Bruker Ultra-Shield (AVANCE III). Fluorescence spectra were recorded on H4 Synergy Microplate Reader (BioTek, USA) and

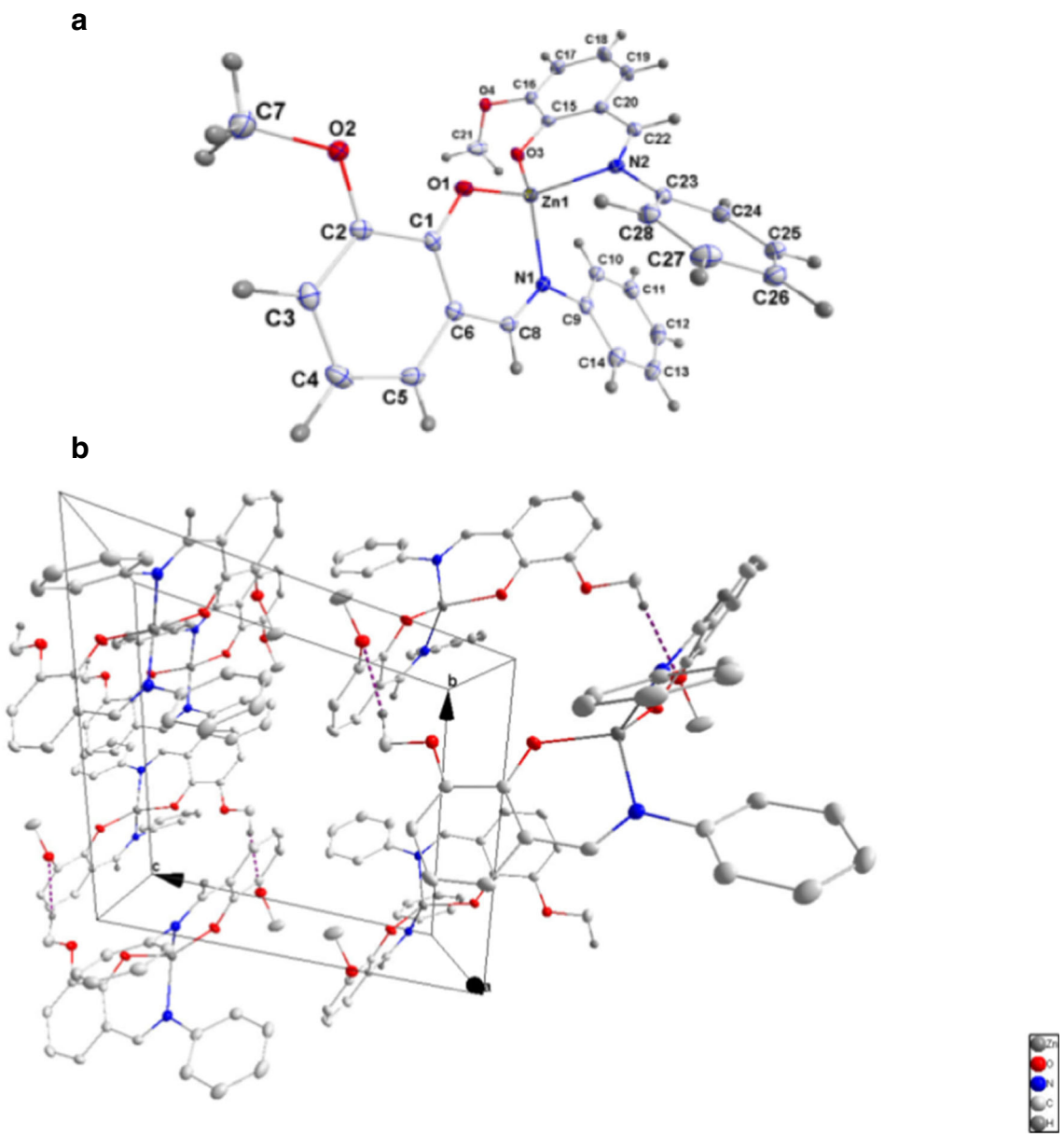

Fig. 1 **a** ORTEP diagram of the complex [Zn complex]. Displacement ellipsoids are drawn at the 50 % probability level **b** Packing diagram of the complex [Zn complex]

Hitachi F-2700 FL Spectrophotometer, UV-Vis absorption spectra were recorded on a Shimadzu UV-1650 PC.

Preparation of Ligand and Complexes

Preparation of the Ligand (HL)

The ligand (HL) was synthesized by refluxing mixture of 1:1 mol ratio *o*-vanillin and aniline in absolute ethanol for 5 h. After cooling down to room temperature (RT), the orange-red precipitate was filtered and washed with cold absolute ethanol. M.p.: 68–70 °C, FT-IR (KBr cm^{-1}, w, weak; s, strong): 1615 (s, $\upsilon_{C=N}$), 1588 (s, $\upsilon_{C=C}$), 1270 (s, υ_{C-O}) [9].

Preparation of bis(2-Methoxy-6-((Phenylimino)Methyl) Phenolato)- Zinc(II) (Zn Complex) Complex

$Zn(OAc)_2$ (0.043 g, 0.2 mmol) in 5 mL absolute methanol was added dropwise to a methanol solution (10 mL) of HL (0.09 g, 0.4 mmol). The mixture was stirred for 24 h at 40 °C. After 3 days at RT, product was refrigerated at 4 °C for 5 more days, and then yellow-orange precipitate was filtered and washed with cold absolute ethanol. The solid residue was crystallized

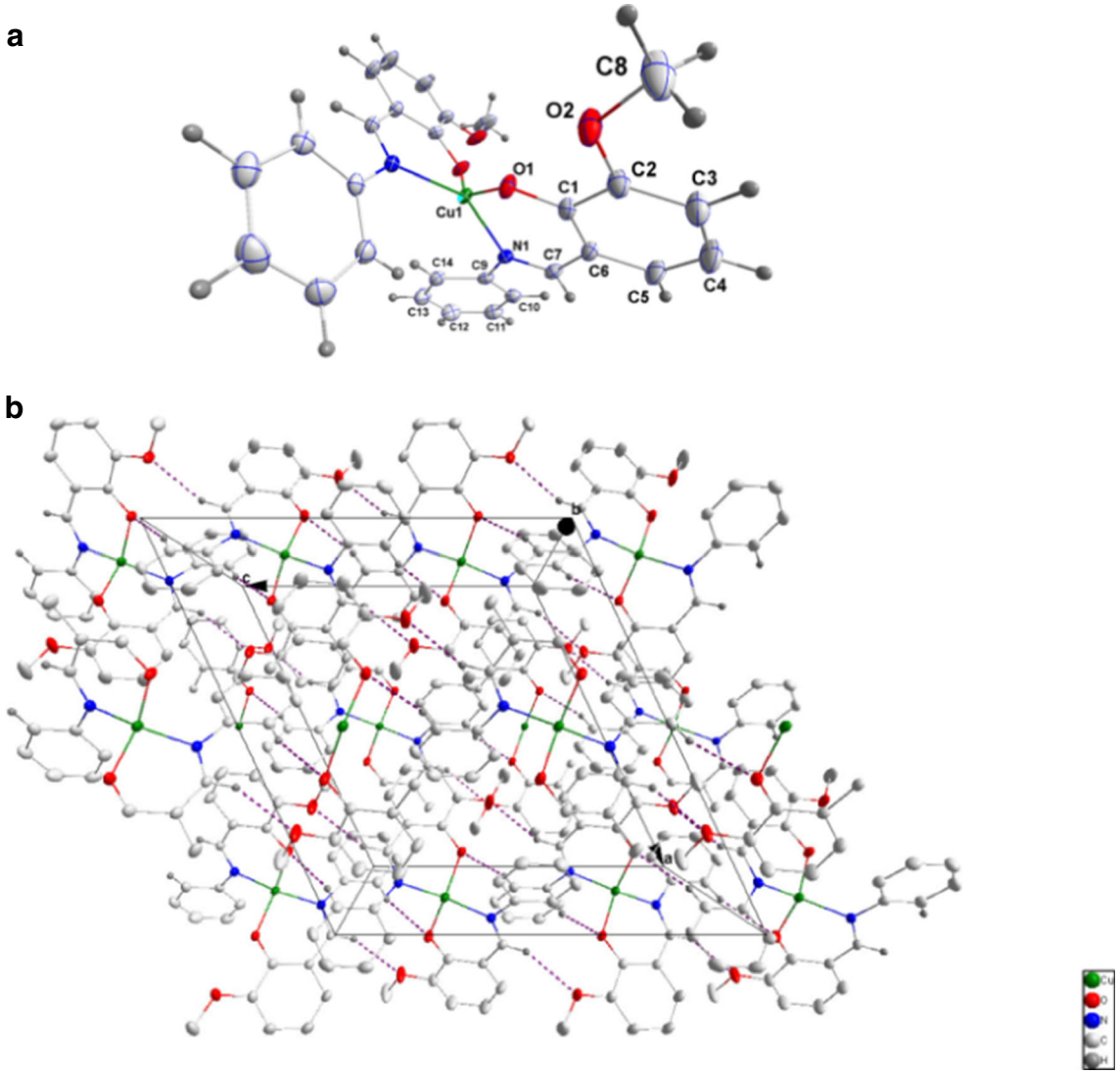

Fig. 2 **a** ORTEP diagram of the complex [Cu complex] Displacement ellipsoids are drawn at the 50 % probability level for non-hydrogen atoms. **b** Packing diagram of the complex [Cu complex]

by diffusion of ether into chloroform solution. M.p.: 249–251 °C, Anal. Calc. % for $C_{28}H_{24}N_2O_4Zn$ (517.86): C 64.94; H 4.73; N 5.64: Found C 64.86; H 4.73; N 5.64 %. ^{1}H NMR: ($CDCl_3$) δ 3.92 (s, 3 H), 6.62 (t, 1 H, j = 3 Hz), 6.82–6.86 (dd, 1 H, j_1 = 7, j_2 = 1 Hz), 6.94–6.97 (dd, 1 H, j_1 = 6, j_2 = 1 Hz), 7.02 (d, 1 H, j = 7 Hz), 7.16–7.24 (m, 3 H), 8.32 (s, 3 H). FT-IR (KBr cm^{-1}, w, weak; s, strong): 1608 (s, $\upsilon_{C=N}$), 1587 (s, $\upsilon_{C=C}$), 1231 (s, υ_{C-O}).

Preparation of bis(2-Methoxy-6-((Phenylimino)methyl) phenolato)- Copper(II) (Cu Complex) Complex

$Cu(OAc)_2$ (0.04 g, 0.2 mmol) in 5 mL absolute methanol was added to a 10 mL methanolic solution of HL (0.09 g, 0.4 mmol). The reaction mixture was refluxed for 4 h. After cooling down to 4 °C, the precipitate was filtered and washed with cold absolute methanol. The solid residue was crystallized from dichloromethane and 2-propanol mixture. M.p.: 197–199 °C, Anal. Calc. % for $C_{28}H_{24}N_2O_4Cu$ (516.03): C 65.17; H 4.68; N 5.42, Found: C 65.24; H 4.75; N 5.70. FT-IR (KBr cm^{-1}): 1606 (s, $\upsilon_{C=N}$), 1587 (s, $\upsilon_{C=C}$), 1231(s, υ_{C-O}).

X-Ray Crystallography

A yellow plate-like single crystal of $C_{28}H_{24}N_2O_4Zn$, approximate dimensions 0.050 mm × 0.140 mm × 0.210 mm and a dark orange plate-like single crystal of $C_{28}H_{24}CuN_2O_4$, approximate dimensions 0.056 mm × 0.170 mm × 0.200 mm, were used for the X-ray crystallographic analysis. The diffraction data for Zn complex was collected using a Bruker D8 VENTURE PHOTON 100 CMOS, using mirror-monochoromated Cu- Kα radiation (λ = 1.54178 Å) in φ

and ω scan at 150(2) K. and the diffraction data for Cu complex was collected on a Bruker Smart APEX CCD, using graphite- monochoromated Mo-Kα radiation (λ = 0.71073 Å) in φ and ω scan at 150(2) (Zn complex) and 98(2) (Cu complex) K. Structures were solved by direct methods and refined on F^2 by full-matrix least-squares methods using the SHELXL-2013 program [24]. Multi-scan method (SADABS) was performed for absorption correction. H-atoms were placed in calculated positions and included as riding contributions with isotropic displacement parameters 1.2–1.5 times those of the attached carbon atoms. CCDC reference numbers for Zn complex and Cu complex are 974,984 and 974,985, respectively.

Photophysical Properties

Fluorescence properties of synthesized complex were recorded in dimethylsulfoxide (DMSO), dimethylformamide (DMF), CH_3OH, C_2H_5OH and acetonitrile solvents at RT. Also the fluorescence emission spectrum of Zn complex was compared with HL with the same concentrations in DMSO solvent. The fluorescence quantum yields of the Zn complex was calculated using fluorescein as reference compound [25].

Interaction of Zn Complex with DNA

UV-Visible Spectroscopy

Zn complex complex was dissolved in 2.5 % DMSO solution to final concentration of 50 μM. 2.5 % DMSO was used as blank in all experiment. Final DNA concentration ranging from 0 to 75 μM were added to constant amount of complex and UV-Vis spectra were recorded on a Shimadzu UV-1650 PC spectrophotometer using a 1.0 cm cell.

Fluorescence Studies

pTZ57R plasmids were purified from transformed *E. coli* using Mini Prep. (Plasmid Purification kit, ThermoScience, USA). Zn and Cu complexes in DMSO were titrated with aqueous solution of plasmids, and the fluorescence intensities were recorded.

Ethidium Bromide Displacement

ncreasing final concentrations of Zn complex complex, from 0 to 100 fold of ethidium bromide (EB) concentration, were added to EB-DNA and its emission spectra from 550 to 700 nm (λ_{Ex} = 526 nm) was recorded. A solution with DMSO concentration the same as corresponding ligand complex solution was used as control.

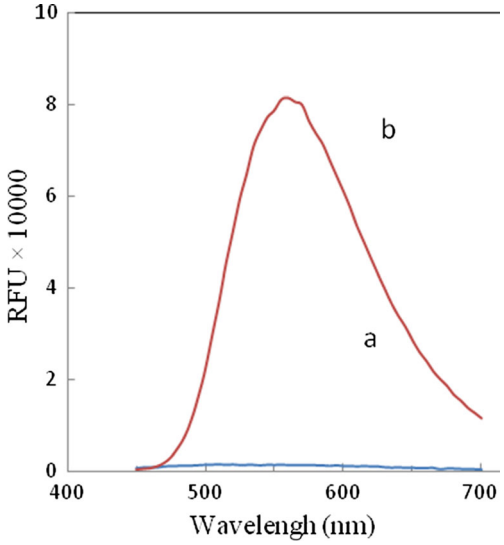

Fig. 3 Fluorescence spectra of Zn (II) complex and Ligand HL at the same concentrations. **a** ligand **b** Zn complex

Viscosity

To further clarify the mechanism of interaction between complex and DNA, the relative viscosity studies were performed. Briefly, 5 mL of 60 μM DNA was mixed with complex ranging from 0.0–130 μM Zn complex (final concentration) at 23 °C, and flow time was measured using digital stop watch each measurement was repeated for 4 times. Relative viscosity in presence and absence of Zn complex was calculated using Eq. 1.

$$\eta/\eta_0 = t/t_0 \quad (1)$$

where η and η_0 were the viscosity of DNA in the presence and absence of the Zn complex complex, respectively [26].

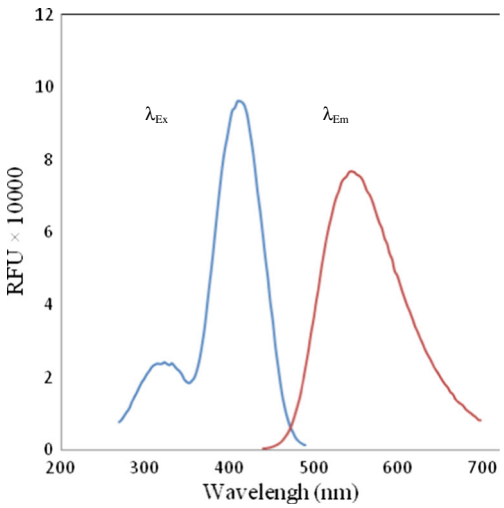

Fig. 4 Determination of excitation and emission wavelength for Zn complex (96 μM) in DMSO)

Table 3 λ_{Ex}, λ_{Em}, and relative fluorescence unit for Zn complex in various solvents

Solvent	Ex	Em	RFU
DMF	412	554	39,163
DMSO	420	560	56,328
Ethanol	414	540	26,566
Methanol	408	540	42,560
Acetonitryl	416	546	22,606

RFU relative fluorescence units

MTT Assay

The cytotoxicity of the complex was tested in MCF-7 breast cancer cells. Briefly, 1×10^4 cells/well was seeded in 96-well plate. 100, 200, 300, 400, 500 nM and 100, 200, 300, 400 and 500 μM Zn complex were added to each well and incubated for 24 h and 48 h in RPMI cell culture medium in humidified atmosphere with 5 % CO_2 at 37 °C. Then, 20 μL MTT (3-(4, 5-dimethylthiazol-2-yl)-2,5-diphenyltetrazolium bromide) solution was added to each well and mixed. After 3.5 h of incubation medium was removed and 200 μL DMSO was added to each well to dissolve formed formazan and absorbance was measured at λ_{570} nm [27, 28].

Agarose gel Staining

2 mg of Zn complex was dissolved in a 10 mL solution containing 60 % DMSO (dimethylsulfoxide) and 40 % TBE (tris buffered EDTA solution, 1×, pH = 8). Agarose gel was incubated with Zn staining solution for 20 min. at room temperature with gentle shaking in dark. For ethidium bromide, 3 μL of 10 mg/mL solution was added to 10 mL of TBE solution, and incubated for 30 min. at room temperature with gentle shaking in dark [29].

Table 4 Photophysical properties of Zn complex

	λ_{Ex}	λ_{Em}	Φ_F %
HL	403	508	
Zn complex	420	560	0.014

This data were obtain at DMSO

Results and Discussion

Infrared Spectroscopy

For HL ligand, the IR bands in 1614 and 1270 cm^{-1} were attributed to the υ(C = N) and υ(C-O), respectively (Fig. S1). In Zn and Cu complexes, these bands were shifted to lower frequencies around 1607, 1606 and 1244 and 1247 cm^{-1}, respectively. These band shifts could confirm the coordination of imine nitrogen and phenolic oxygen to the center metal ions [5, 9]. IR spectrum of Zn and Cu complexes were provided in supplementary information (Figs. S2 and S3).

NMR Spectroscopy

^{1}H NMR spectrum of Zn complex was recorded in $CDCl_3$. Chemical shift values in spectra was in good agreement with the shifts that has already been reported in the literature for HL ligand [9]. In ^{1}H NMR spectra, there were two indicators signal each appeared as a singlet at δ = 3.92 and 8.325 ppm that were attributed to the OCH_3 and CH = N, respectively [5]. The signals in region δ = 6.598–7.291 were due to the aromatic protons. In the ligand, there is a signal as a singlet at δ = 13.76 ppm but this signal disappear in Zn complex spectra (Figs. S4 and S5).

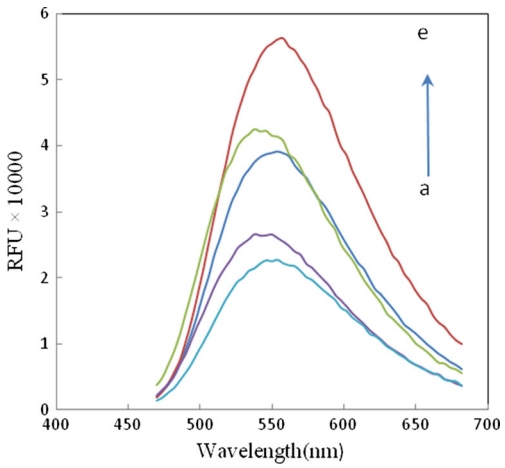

Fig. 5 The emission spectra of Zn complex 76 μM in various solvents. **a** Acetonitrile **b** Ethanol **c** Methanol **d** DMF **e** DMSO

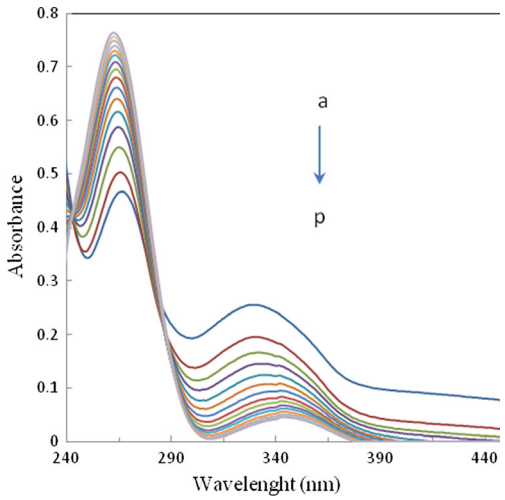

Fig. 6 The UV-Vis absorption spectra of Zn complex (50 μM) in the absence and presence of DNA in 2.5 % DMSO solution (0–75 μM)

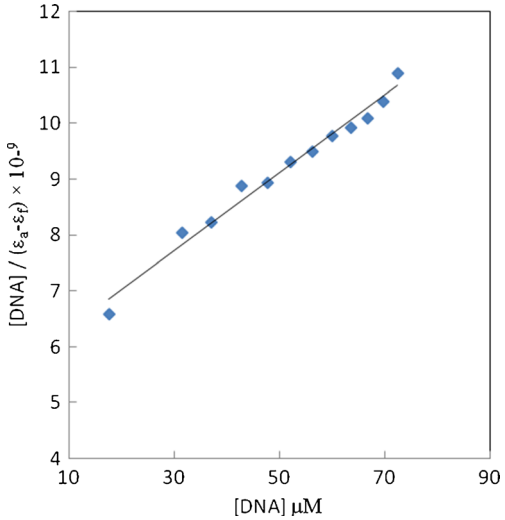

Fig. 7 Plot of [DNA]/(ε_a– ε_b) vs. [DNA] for titration of 50 μM Zn complex with DNA (0–75 μM) at 329 nm

X-ray Structure Characterization

Crystallography data for the Cu complex and Zn complex were presented in Table 1 and the selected bond lengths and bond angles were listed in Table 2.

Each asymmetric unit of Zn and Cu complexes contain one independent molecule and half of a molecule per unit cell, respectively. In each complex, Zn and Cu are coordinated by two oxygen atoms of phenoxide and two nitrogen atoms of imine. Zn complex was crystallized in the triclinic crystal system with *P*-1 space group. The coordination geometry at the metal center could be described as slightly distorted square planar and tetrahedral geometries with a parameter τ_4, $\tau_4 = 0$ and 1 for perfect square planar and perfect tetrahedral geometries, respectively. The τ_4 value of 0.78 [$\tau_4 = (360° - (\alpha + \beta))/141°$, where α = O(3)-Zn(1)-N(1) = 128.03°, β = O(1)-Zn(1)-N(2) = 121.57°] for Zn complex could reflect that the four-coordinate geometry around Zn(II) was close to tetrahedral [30, 31]. In Zn complex, there were two hydrogen bonds between oxygen of methoxy group and H from other methoxy group and hydrogen of imine carbon with oxygen of methoxy group as C7-H7B···O4 and C22-H22···O2 with the distances of 3.462(3) and 3.296(2), respectively (Fig. 1). It is worth to mentioning here that in the crystal structure of the complex there were some non-covalent interactions such as H(4)…H(21)C, C(6)…C(6), and C(1)…C(8) with the distances of 2.259, 2.265 and 3.380 Å, respectively.

Cu complex was crystallized in the monoclinic crystal system with *C*2/*c* space group. The τ_4 value of 0.48 [where α = N(1)-Cu(1)-N(1) = 149.25°, β = O(1)-Cu(1)-O(1) = 141.74°] for Cu complex could indicate the four-coordinate geometry around Cu(II) was close to square planar [30, 31].The Cu-N and Cu-O distances were 1.9585(12) and 1.8984(11) A°, respectively. In Cu complex, there were hydrogen bonds between aromatic hydrogen and oxygen of methoxy group and hydrogen of imine carbon with phenolic oxygen in the same ligand as (Fig. 2), and also in this complex there were some non-covalent interactions such as H(8)C…H(10), H(3)…C(9) and C(7)…C(10) with the distances of 2.844, 2.872, 3.231 Å, respectively.

Fluorescence Studies

Fluorescence properties of synthesized Cu and Zn complexes were studied. Only a weak emission was recorded for the Cu complex in DMF, showing that Cu may quench the ligand. At the same condition, Zn interaction with the ligand could significantly increase the emission intensity. Moreover, Zn complex showed a red shift, and also increased the difference between excitation and emission wave lengths and compared with ligand alone (Fig. 3). The excitation and emission spectrum was shown in Fig. 4. λ_{Ex}, λ_{Em} and Relative Fluorescence Units (RFU) of Zn complex in several solvents have been listed in Table 3. According our data, Zn complex in DMSO

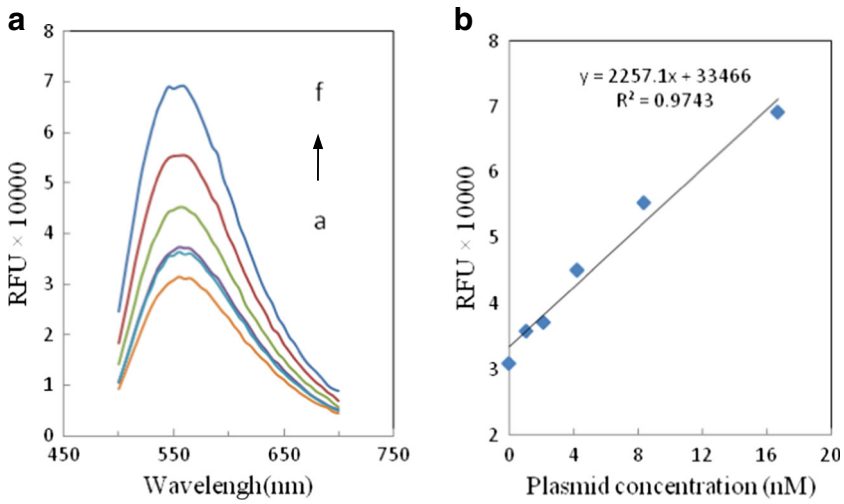

Fig. 8 **a** Fluorescence spectra of Zn complex in the absence and presence of increasing amount of plasmid concentration in DMSO ([DNA], a = 0, b = 5.22×10^{-4}, c = 1.04×10^{-3}, d = 2.09×10^{-3}, e = 4.18×10^{-3}, f = 8.36×10^{-3} μM). **b** Correlation between plasmid concentration and fluorescence intensity of Zn complex

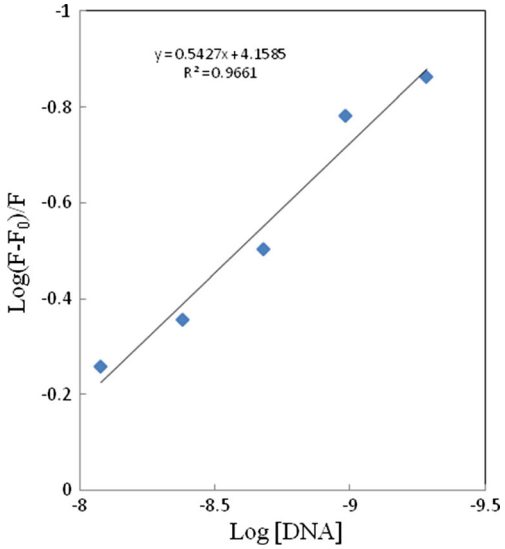

Fig. 9 Plot of log(F-F_0)/F vs. log [DNA]

showed the highest emission intensity (Fig. 5). Although emission in DMF was notable, DMSO was selected for next experiments because of its lower toxicity in biological experiments [32]. The fluorescence quantum yield of the Zn complex was calculated to be 0.014 % (Table 4).

Interaction of Zn Complex with DNA

UV-Vis Absorption Studies

Interaction of Zn complex complex with salmon sperm DNA was also studied by UV-Vis absorption titration. Figure 6 shows the absorption spectra of Zn complex complex in the absence and presence of DNA. The spectra of the free complex were characterized by a peak at 329 nm. Upon addition of DNA, a red shift from 329 nm to 342 nm was recorded. Moreover, increase in A_{262} could be due to • - •* transitions of DNA base.

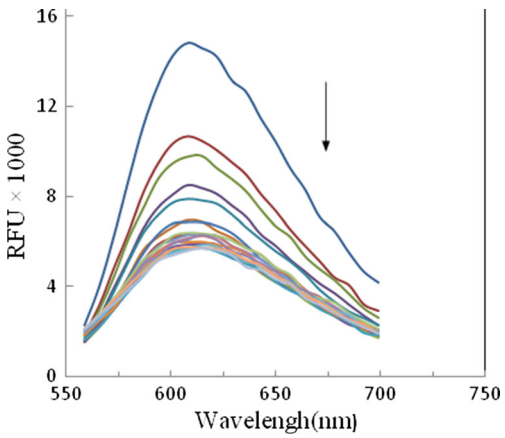

Fig. 10 Fluorescence spectra of DNA-EB system in the presence of Zn complex (λ_{Ex} = 526 nm, λ_{Em} = 605 nm). [DNA] = 3 × 10^{-5} M; [EB] = 5 × 10^{-6} M; [Zn complex] = 4 × 10^{-5} – 6.4 × 10^{-4}

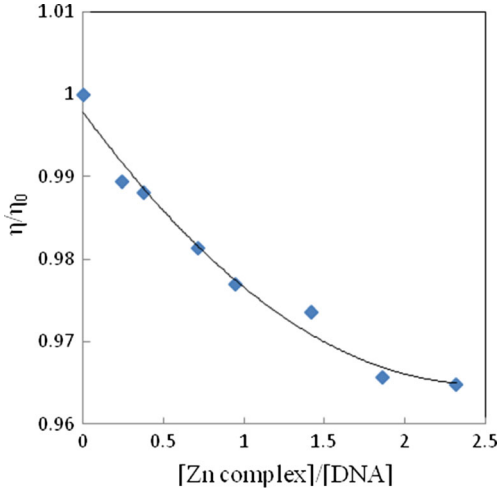

Fig. 11 Effect of increasing amount of the Zn complex (0-137 μM) on relative viscosity DNA. [DNA] = 6 × 10^{-5} M

The hypochromic and bathochromic shifts in Zn complex complex absorption may be observed in both intercalative or groove binding [33, 34]. Binding constant (K_b) for Zn complex with DNA was calculated using the following equation [26].

$$\frac{[DNA]}{\varepsilon_a - \varepsilon_f} = \frac{[DNA]}{\varepsilon_b - \varepsilon_f} + \frac{1}{K_b(\varepsilon_b - \varepsilon_f)} \quad (2)$$

Where [DNA] is the concentration of DNA base pairs, ε_a, ε_f and ε_b correspond to the excitation coefficients for each addition of DNA to the complex, free complex and for the compound in the fully bound form, respectively. The binding constant K_b was calculated from the plot of [DNA]/(ε_a- ε_f) vs. [DNA] and calculated to be 1.16× 10^4 M^{-1} which was smaller than those observed for the DNA classical intercalating agents (10^7–10^9 M^{-1}) and was close to DNA groove binding agents (1.1 × 10^4–4.8 × 10^4 M^{-1}) (Fig. 7) [26].

Fluorescence Spectroscopic Study of the Interaction Between Zn Complex and DNA

As shown in Fig. 8 fluorescence intensity increases linearly as higher concentration of plasmids were used. Equation 3 was used to calculate Zn complex-DNA binding constant and number of binding sites.

$$\text{Log}\left((F_0 - F)/F\right) = \text{logK} + \text{nlog[DNA]} \quad (3)$$

Table 5 IC_{50} values obtain for the Zn complex against MCF-7 cells

Complex	IC_{50}	
	24 h	48 h
Zn complex	322.80 μM	250.28 μM

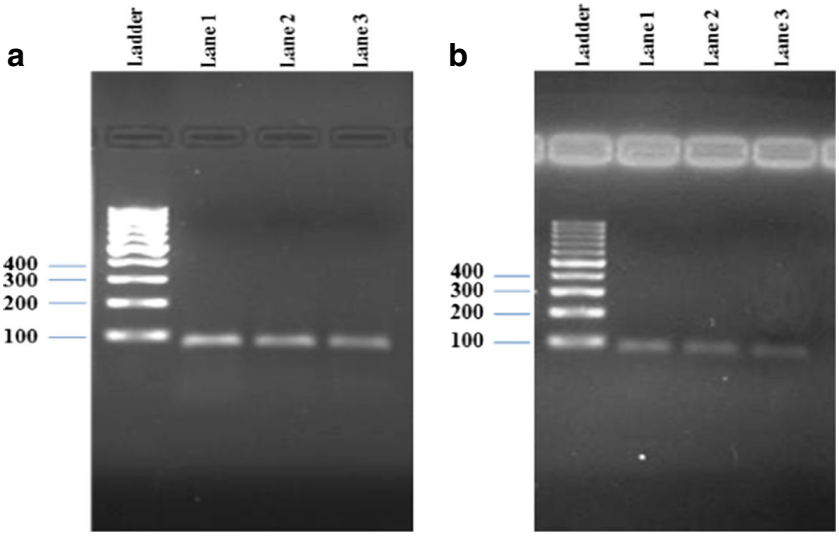

Fig. 12 **a** Agarose gel staining with Ethydium bromid, ladder 100 bp, (lane 1)30 μL, (lane 2) 20 μL, (lane 3) 10 μL of 80 bp PCR production **b** Agarose gel staining with Zn complex, (lane 1)30 μL, (lane 2) 20 μL, (lane 3) 10 μL of 80 bp PCR production

F_0 and F are the fluorescence of the fluorophore in the absence and presence of different concentration of DNA respectively, K is binding constant and n is number of binding sites [35]. As in our experiment $F > F_0$, equation was modified as Eq. 4 [34].

$$\text{Log}\left((F-F_0)/F\right) = \text{logK} + \text{nlog[DNA]} \quad (4)$$

K and n for Zn complex were calculated to be 1.44×10^4 M^{-1} and 0.5, respectively (Fig. 9). The calculated K was 100 time less than K for known intercalating agent like ethidium bromide ($K = 2.6 \times 10^6$), so we concluded that binding of Zn complex to DNA could not be through intercalation [34, 35].

DNA-Binding Competition Between Ethidium Bromide and Zn Complex Complex

Ethidium bromide is a DNA intercalating compound and is used as a probe to study the interaction of small molecules with double-stranded DNA [35]. Emission of ethidium bromide increases upon its interaction with dsDNA. As λ_{Ex} (525 nm) and λ_{Em} (600 nm) of ethidium bromide are quite different from those (λ_{Ex} = 420 nm and λ_{Em} = 560 nm) in Zn complex, we successfully used emission intensities to monitor Zn complex interaction with DNA [19]. Aqueous solution of DNA-EB complex was titrated with Zn complex. Figure 10 shows the emission profile of DNA-EB in the absence and presence of different concentrations of Zn complex. Fluorescence intensities of EB decreased as higher amounts of Zn complex was added to the solution.

Binding constant was calculated using the equation K_{EB} $C_{EB} = K_{app}$ $C_{50complex}$. Where $K_{EB} = 1 \times 10^7 M^{-1}$, $C_{EB} = 5 \times 10^6$ M, K_{app} is apparent binding constant and $C_{50\ complex}$ is value of complex at 50 % reduction of the fluorescence intensity of EB [33].

Although we increased the concentration of Zn complex up to 100 fold more that EB concentration, fluorescence intensity decreased to about 50 %. So that, based on the Eq. 1, it was concluded that the apparent binding constant for Zn complex should be less than 10^5, which is much lower than K for known intercalating agents [8].

Viscosity

Classical intercalating agents unwind the DNA helix, so that increase the length of DNA. As viscosity is directly related to the length of DNA, intercalation to the small molecules

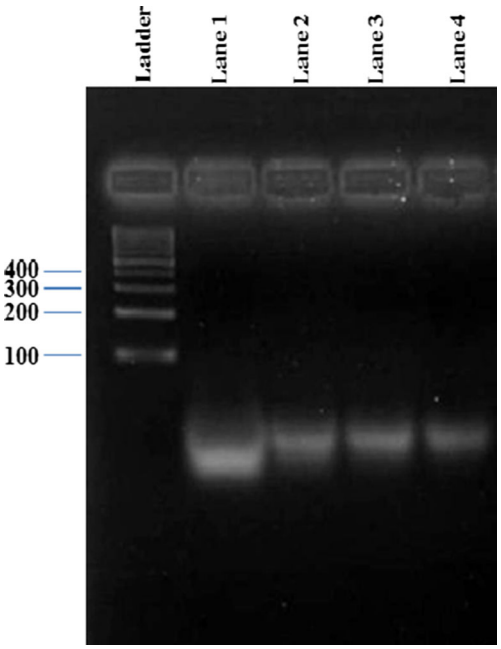

Fig. 13 Agarose gel staining with Ethydium bromid, ladder 100 bp, (lane 1) 0.62 nM, (lane 2) 0.41 nM, (lane 3) 0.21 nM and (lane 4) o.12 nM of 40 bases ssDNA, that synthesized with DNA synthesizer

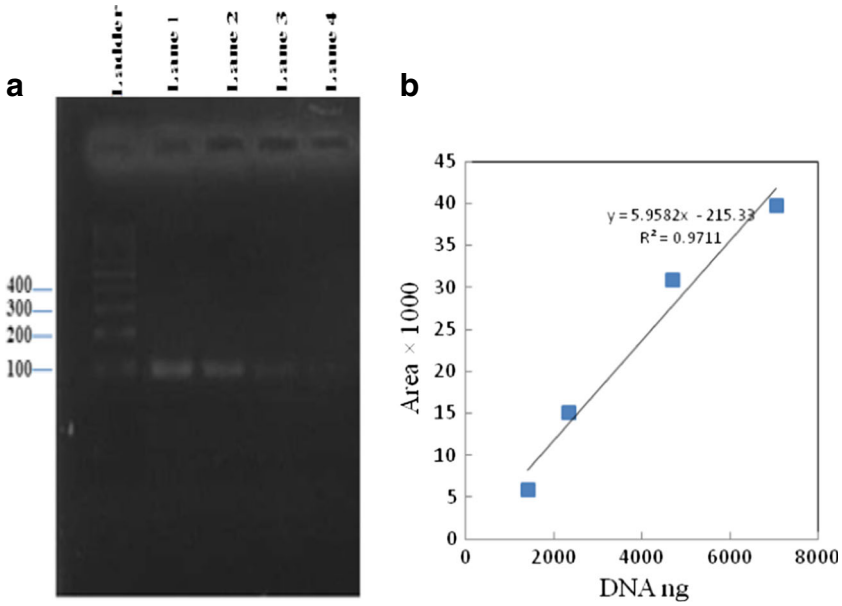

Fig. 14 **a** 80 bp PCR product were loaded onto 2 % agarose gel, (lane 1) 7.05, (lane 2) 4.70, (lane 3) 2.35 and (lane 4) 1.41 μg/mL. **b** Image intensity across the gel from 7.05–1.41 μg/mL product PCR

increases the viscosity of DNA solution. As shown in Fig. 11, relative viscosity of DNA solution did not increase upon addition of complex; so that we concluded that interaction of complex with DNA in not through classical intercalation [26, 33].

MTT Assay

Cytotoxicity of Zn complex against the MCF-7 cell line was studied. IC_{50} was calculated to be 322.80 μM (Table 5). Compared to known cytotoxic compounds like ethidium bromide (200 nM and Doxorubicin (10 nM), our newly synthesized compound was much less toxic [36, 37].

Staining of Agarose gel with Zn Complex and Ethidium Bromide

Ethidium bromide, as an intercalating fluorescent probe, can be used to stain and detect low amount of double stranded DNA in agarose gel. Mutagenicity and cytotoxicity of ethidium bromide are drawbacks to its application in lab. As we detect a very sharp increase in fluorescence intensity of Zn complex upon binding to DNA, potential application of this complex in staining of single and double stranded DNA in agarose gel was examined. 80 bp PCR product and 40 bases synthetic ssDNA were loaded onto 2 % agarose gels. As shown in Figs. 12b and 13. Zn complex could successfully be used to stain both gels, although staining with ethidium bromide (Fig. 12a) was more efficient. We showed that there was a linear correlation between band intensities and amount of loaded PCR products (Fig. 14) [38].

Conclusion

In this context, we synthesized and characterized two new complexes, *bis*(2-methoxy-6-((phenylimino) methyl)phenolato)- zinc(II) and a *bis*(2-methoxy-6-((phenylimino)methyl)phenolato)- copper(II). Fluorescence properties of these compounds in several solvents were investigated and the quantum yield of Zn complex in DMSO was calculated to be 0.014 %. We showed that Zn complex interaction with dsDNA was through groove binding, and also accompanied with significant increase in its fluorescence intensity, $K_b = 10^4\ M^{-1}$, making it a good candidate as a probe for the detection of DNA. We also showed that Zn complex did not have a significant impact on MCF7 cell line viability in nano molar concentrations. Moreover, we successfully stained both ssDNA and dsDNA in agarose gel using Zn complex.

DMSO Dimethylsulfoxide, *DMF* Dimethylformamide, *EB* Ethidium bromide, *MCF-7* Michigan Cancer Foundation-7, *MTT* 3-(4,5-dimethylthiazol-2-yl)-2, 5-diphenyltetrazolium Bromide, *RFU* Relative fluorescence units, IC_{50} half maximal (50 %) inhibitory concentration (IC) of a substances

Acknowledgments The Research Council of Ferdowsi University of Mashhad is acknowledged for financial support (Grant No. 3/26199). Thanks to Dr. Sattar Saberi for his constructive comments. The support of NSF-MRI Grant #1228232 for the purchase of the diffractometer is gratefully acknowledged.

References

1. Coles S, Hursthouse M, Kelly D, Toner A, Walker N (1998) Halide titanium (IV) Schiff base complexes; fluoride and bromide

derivatives and evidence for a new seven-coordinate chloride intermediate. J Chem Soc Dalton Trans :3489–3494
2. Mohammadi K, Niad M, Jafari T (2014) New 3, 4-diaminobenzoic acid Schiff base compounds and their complexes: synthesis, characterization and thermodynamics. Spectrochim Acta Part A 122: 179–185
3. Ji Y-F, Wang R, Ding S, Du C-F, Liu Z-L (2012) Synthesis, crystal structures and fluorescence studies of three new Zn (II) complexes with multidentate Schiff base ligands. Inorg Chem Commun 16:47–50
4. Anupama B, Sunita M, Leela DS, Ushaiah B, Kumari CG (2014) Synthesis, spectral characterization, DNA binding studies and antimicrobial activity of Co (II), Ni (II), Zn (II), Fe (III) and VO (IV) complexes with 4-aminoantipyrine schiff base of ortho-vanillin. J Fluoresc 24:1067–1076
5. Mendu P, Kumari CG, Ragi R (2015) Synthesis, characterization, DNA binding, DNA cleavage and antimicrobial studies of Schiff base ligand and its metal complexes. J Fluoresc 25:369–378
6. Li P, Niu M, Hong M, Cheng S, Dou J (2014) Effect of structure and composition of nickel(II) complexes with salicylidene Schiff base ligands on their DNA/protein interaction and cytotoxicity. J Inorg Biochem 137:101–108
7. Ma Z-Y, Qiao X, Xie C-Z, Shao J, Xu J-Y, Qiang Z-Y, Lou J-S (2012) Activities of a novel Schiff Base copper (II) complex on growth inhibition and apoptosis induction toward MCF-7 human breast cancer cells via mitochondrial pathway. J Inorg Biochem 117:1–9
8. Qiao X, Ma Z-Y, Xie C-Z, Xue F, Zhang Y-W, Xu J-Y, Qiang Z-Y, Lou J-S, Chen G-J, Yan S-P (2011) Study on potential antitumor mechanism of a novel Schiff Base copper (II) complex: synthesis, crystal structure, DNA binding, cytotoxicity and apoptosis induction activity. J Inorg Biochem 105:728–737
9. Yeap G-Y, Ha S-T, Ishizawa N, Suda K, Boey P-L, Kamil Mahmood WA (2003) Synthesis, crystal structure and spectroscopic study of para substituted 2-hydroxy-3-methoxybenzalideneanilines. J Mol Struct 658:87–99
10. Zhang Y-G, Shi Z-H, Yang L-Z, Tang X-L, An Y-Q, Ju Z-H, Liu W-S (2014) A facile fluorescent probe based on coumarin-derived Schiff base for Al^{3+} in aqueous media. Inorg Chem Commun 39: 86–89
11. Niu S, Zhao M, Ren R, Zhang S (2009) Carbon nanotube-enhanced DNA biosensor for DNA hybridization detection using manganese (II)â€“Schiff base complex as hybridization indicator. J Inorg Biochem 103:43–49
12. Kotova OV, Eliseeva SV, Averjushkin AS, Lepnev LS, Vaschenko AA, Rogachev AY, Vitukhnovskii AG, Kuzmina NP (2008) Zinc (II) complexes with Schiff bases derived from ethylenediamine and salicylaldehyde: the synthesis and photoluminescent properties. Russ Chem Bull Int Ed 57:1880–1889
13. van Wyk JL, Mapolie S, Lennartson A, Hakansson M, Jagner S (2007) The synthesis of copper (II) salicylaldiminato complexes and their catalytic activity in the hydroxylation of phenol. Z Naturforsch B 62b:331
14. Zou D, Feng W, Shi G, Lü X, Zhang Z, Zhang Y, Liu H, Fan D, Wong W-K, Jones RA (2012) Hetero-binuclear near-infrared (NIR) luminescent Zn–Nd complexes self-assembled from the benzimidazole-based ligands. Spectrochim Acta Part A 98:359–366
15. Mandal S, Modak R, Goswami S (2013) Synthesis and characterization of a copper (II) complex of a ONN donor Schiff base ligand derived from pyridoxal and 2-(pyrid-2-yl) ethylamine–A novel pyridoxal based fluorescent probe. J Mol Struct 1037:352–360
16. Zhang G, Guo J, Zhao N, Wang J (2010) Study of interaction between kaempferol–Eu^{3+} complex and DNA with the use of the neutral red dye as a fluorescence probe. Sensors Actuators B Chem 144:239–246
17. Ahmadi SM, Dehghan G, Hosseinpourfeizi MA, Dolatabadi JEN, Kashanian S (2011) Preparation, characterization, and DNA binding studies of water-soluble quercetin–molybdenum (VI) complex. DNA Cell Biol 30:517–523
18. Kashanian S, Khodaei MM, Pakravan P, Adibi H (2012) Molecular aspects on the interaction of isatin-3-isonicotinylhydrazone to deoxyribonucleic acid: model for intercalative drug-DNA binding. Mol Biol Rep 39:3853–3861
19. Yegorova A, Karasyov A, Duerkop A, Ukrainets I, Antonovich V (2005) New luminescent terbium complex for the determination of DNA. Spectrochim Acta Part A 61:109–116
20. Holmlin RE, Yao JA, Barton JK (1999) Dipyridophenazine complexes of Os (II) as red-emitting DNA probes: synthesis, characterization, and photophysical properties. Inorg Chem 38:174–189
21. Wang YT, Zhao FL, Li KA, Tong SY (1999) Molecular spectroscopic study of DNA binding with neutral red and application to assay of nucleic acids. Anal Chim Acta 396:75–81
22. Rajendiran V, Palaniandavar M, Periasamy VS, Akbarsha MA (2010) $[Ru(phen)_2(dppz)]^{2+}$ as an efficient optical probe for staining nuclear components. J Inorg Biochem 104:217–220
23. Keller M, Erdmann D, Pop N, Pluym N, Teng S, Bernhardt G, Buschauer A (2011) Red-fluorescent argininamide-type NPY Y_1 receptor antagonists as pharmacological tools. Bioorgan Med Chem 19:2859–2878
24. Sheldrick G (2013) SHELXL-2013. University of Göttingen, Göttingen
25. Brouwer AM (2011) Standards for photoluminescence quantum yield measurements in solution (IUPAC technical report). Pure Appl Chem 83:2213–2228
26. Rad FV, Housaindokht MR, Jalal R, Hosseini HE, Doghaei AV, Goghari SS (2014) Spectroscopic and molecular modeling based approaches to study on the binding behavior of DNA with a copper (II) complex. J Fluoresc 24:1225–1234
27. Zhao X, Lee PP-F, Yan Y-K, Chu C-K (2007) Synthesis, crystal structures and cytotoxicities of some transition metal complexes with N-[2-{(pyridin-2- ylmethylidene)amino}ethyl]acetamide. J Inorg Biochem 101:321–328
28. Taghdisi SM, Lavaee P, Ramezani M, Abnous K (2011) Reversible targeting and controlled release delivery of daunorubicin to cancer cells by aptamer-wrapped carbon nanotubes. Eur J Pharm Biopharm 77:200–206
29. Tuma RS, Beaudet MP, Jin X, Jones LJ, Cheung C-Y, Yue S, Singer VL (1999) Characterization of SYBR gold nucleic acid gel stain: a dye optimized for use with 300-nm ultraviolet transilluminators. Anal Biochem 268:278–288
30. Yang L, Powell DR, Houser RP (2007) Structural variation in copper (I) complexes with pyridylmethylamide ligands: structural analysis with a new four-coordinate geometry index, τ_4. Dalton Trans 955-964
31. García-Giménez JL, Hernández-Gil J, Martínez-Ruíz A, Castiñeiras A, Liu-González M, Pallardó FV, Borrás J, Piña GA (2013) DNA binding, nuclease activity, DNA photocleavage and cytotoxic properties of Cu (II) complexes of N-substituted sulfonamides. J Inorg Biochem 121:167–178
32. Ponec M, Haverkort M, Soei YL, Kempenaar J, Bodde H (1990) Use of human keratinocyte and fibroblast cultures for toxicity studies of topically applied compounds. J Pharm Sci 79:312–316
33. Liang J-W, Wang Y, Du K-J, Li G-Y, Guan R-L, Ji L-N, Chao H (2014) Synthesis, DNA interaction and anticancer activity of copper (II) complexes with 4′-phenyl-2, 2′: 6′, 2 ″-terpyridine derivatives. J Inorg Biochem 141:17–27
34. Bera R, Sahoo BK, Ghosh KS, Dasgupta S (2008) Studies on the interaction of isoxazolcurcumin with calf thymus DNA. Int J Biol Macromol 42:14–21

35. Zhang G, Hu X, Zhao N, Li W, He L (2010) Studies on the interaction of aminocarb with calf thymus DNA by spectroscopic methods. Pestic Biochem Phys 98:206–212
36. Panasci L, Jean-Claude BJ, Vosilescu D, Mustafa A, Damian S, Damian Z, Georges E, Liu Z, Batist G, Leyland-Jones B (1996) Sensitization to doxorubicin resistance in breast cancer cell lines by tamoxifen and megestrol acetate. Biochem Pharmacol 52:1097–1102
37. Luedtke NW, Tor Y (2003) Fluorescence-based methods for evaluating the RNA affinity and specificity of HIV-1 Rev–RRE inhibitors. Biopolymers 70:103–119
38. Kiltie AE, Ryan AJ (1997) SYBR green I staining of pulsed field agarose gels is a sensitive and inexpensive way of quantitating DNA double-strand breaks in mammalian cells. Nucleic Acids Res 25:2945–2946